

# NATIONAL AERONAUTICS AND SPACE ADMINISTRATION

TECHNICAL REPORT  
R-134

## AERODYNAMIC EVIDENCE PERTAINING TO THE ENTRY OF TEKTITES INTO THE EARTH'S ATMOSPHERE

By DEAN R. CHAPMAN, HOWARD K. LARSON,  
and LEWIS A. ANDERSON

1962

LOAN COPY: 1  
AFSWC (S  
KIRTLAND A

006822J



TECH LIBRARY KAFB, NM



---

# **TECHNICAL REPORT R-134**

---

## **AERODYNAMIC EVIDENCE PERTAINING TO THE ENTRY OF TEKTITES INTO THE EARTH'S ATMOSPHERE**

**By DEAN R. CHAPMAN, HOWARD K. LARSON,  
and LEWIS A. ANDERSON**

**Ames Research Center  
Moffett Field, Calif.**

## TECHNICAL REPORT R-134

# AERODYNAMIC EVIDENCE PERTAINING TO THE ENTRY OF TEKTITES INTO THE EARTH'S ATMOSPHERE

By DEAN R. CHAPMAN, HOWARD K. LARSON, and LEWIS A. ANDERSON

### SUMMARY

*Evidence is presented which shows that the Australian and Java tektites entered the earth's atmosphere and experienced ablation by severe aerodynamic heating in hypervelocity flight. The laboratory experiments on hypervelocity ablation have reproduced ring-wave flow ridges and coiled circumferential flanges like those found on certain of these tektites. Systematic striae distortions exhibited in a thin layer beneath the front surface of australites also are reproduced in the laboratory ablation experiments, and are shown to correspond to the calculated distortions for aerodynamic ablation of a glass. About 98 percent of Australian tektites represent aerodynamically stable configurations during the ablative portion of an entry trajectory. Certain meteorites exhibit surface features similar to those on tektites.*

### INTRODUCTION

At irregular intervals during the past 170 years, numerous natural glass objects of curious shape and unknown origin have been found scattered over certain geographical areas of the globe. Given the name "tektites," from the Greek word  $\tau\eta\chi\tau\omicron\varsigma$  (meaning "molten"), they long have been the object of detailed study by chemists, geologists, naturalists, geochemists, petrologists, mineralogists, and physicists—but not by aerodynamicists. There are two principal reasons for a belated entry of aerodynamicists into the field of tektite research: First, it has only been in the past few years that a stage of advancement has been reached wherein laboratory facilities have provided an appropriate experimental environment, and theoretical studies an adequate analytical basis, for understanding the hypervelocity ablation of glasses; and, second, the

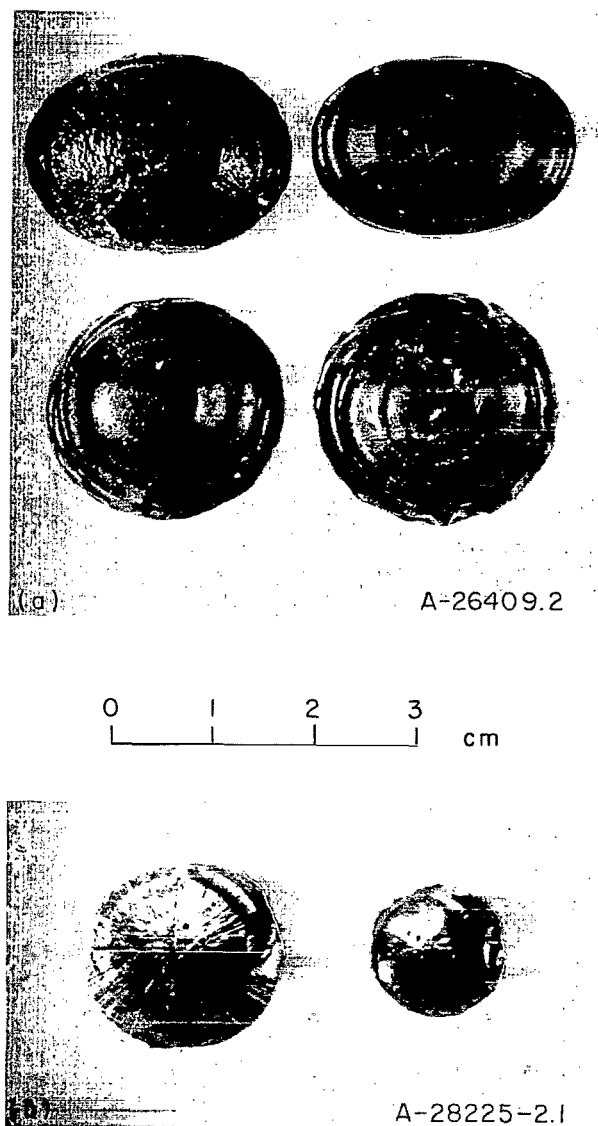
descriptions of various tektites which happen to exhibit unmistakable aerodynamic features have been published in scientific journals that are not normally perused by aerodynamicists. As a net result, atmosphere-entry research on glassy heat shields for missiles and spacecraft has been advancing during the past few years in a spirit oblivious to the existence of tektites, while producing in the process research results which have a crucial bearing on the controversial scientific question of tektite origin.

Curiously enough, glass of tektite composition constitutes a good heat-shield material. Whether this is an accident of nature or a necessity for survival is not clear at present. In either case, circumstances are fortunate in that tektite glass is close in composition to glassy heat-shield materials already extensively studied as part of the re-entry research programs in the United States. Hence a broad backlog of research is now available upon which an experimental and theoretical aerodynamic investigation of tektites can be based.

While experimental information pertaining to atmosphere-entry aerodynamics of tektites has been absent in the past, this has not prevented many fertile minds from offering views as to whether or not the peculiar sculpturing of certain tektites is the result of some aerodynamic action. As in other examples of scientific inquiry wherein an experimental void has made speculation necessary, a variety of conflicting views has been the net outcome. We have on one extreme, for example, a firm view recently stated by Krinov (ref. 1), an eminent student of meteorites, that "In reality there are no traces, even the smallest, of the action of the atmosphere on tektites, their form, surface relief, or structure. The form and surface struc-

ture of tektites decisively show that they are the result of mechanical and chemical erosion." Many years previously, Dunn (ref. 2) expressed similar disbelief that aerodynamic effects could have produced the tektite sculpture. In Dunn's view it was inconceivable that such beautifully symmetric forms as are observed on certain of the Australian button-type tektites could be caused by rapid flight in the atmosphere. (Dunn's tektite collection is now in the British Museum, and four of his australite buttons are shown in the top portion of figure 1.) Urey (ref. 3) has voiced a similar skepticism to that of Dunn in doubting that a small glass object 1 to 2 cm in diameter would travel at high velocity in the atmosphere, keeping one orientation as is necessary in the case of the button-shaped tektites. Analogous doubts that entry aerodynamics has played the leading role in shaping the Australian tektites have been expressed by others: Berwerth (ref. 4), for example, believed that tektites were man-made, suggesting that the spiral ridges on australite buttons were produced by a twisting pressure applied artificially to soft glass; while Watson (ref. 5) calculated that sufficient heat could not possibly be transferred by atmospheric friction to allow the australites to take on their observed shapes; and Hawkins (ref. 6), who favored a lightning origin for tektites, cautioned against what he regarded as an unwarranted assumption that australite forms were produced by aerodynamic effects.

On the other hand, the opposite view that tektite shapes were formed in some way during entry into the atmosphere is also prevalent in the literature. Such views have been expressed by Steltzner (ref. 7), who surmised that the australite ridges and flanges were produced during a non-spinning entry into the atmosphere; by Suess (ref. 8), who regarded the moldavite sculpture as similar to that on meteorites; by Lacroix (ref. 9) and Fenner (ref. 10), who believed the tektites forms to have been produced from aerodynamic action on soft, spinning, ablation drops after they were shed from a larger combustible meteorite; by Von Koenigswald (ref. 11), who pointed to certain features of the Java tektite sculpture as being similar to those on fragmented meteorites; and by O'Keefe (ref. 12), who hypothesized that the australites were formed from a large object which grazed an edge of the earth's atmosphere and shed



(a) Australite buttons; collection of British Museum.

(b) Java tektites; collection of G. H. R. von Koenigswald.

FIGURE 1.—Tektites exhibiting ring-wave flow ridges on their front surfaces.

melted ablation drops in a fashion which enabled them to be trapped in an orbit around the earth, and to land later as tektites. The most detailed views advanced heretofore about the aerodynamic sculpturing of australites, however, have been given by Baker (refs. 13 and 14), who concluded that the most logical and acceptable theory is that the Australian tektite sculpture was formed from cold, nonrotating glass objects that entered the

atmosphere at high velocity and were reshaped by aerodynamic effects from certain original forms (mostly spheres) into their observed shapes. Baker regarded his deductions as qualitative in nature since he believed that aerodynamicists then (1958) had not yet formulated answers to the problems involved.

With benefit of knowledge of some recent researches on the aerodynamic ablation of glasses, a study of australites was made by the senior author in 1959-60. The essential results have been summarized, but not elaborated upon (Chapman, ref. 15), and have led to the conclusions that (1) the surface flow patterns, the internal striae distortion, and the aerodynamically stable shapes of Australian tektites provide an unmistakable record of ablation of a rigid glass during hypervelocity entry into the earth's atmosphere, and that (2) this record is sufficiently complete to deduce the approximate entry velocity, the flight-path angle, and the probable celestial object of tektite origin. The objective of the present report is to present a detailed account of experimental and theoretical evidence pertaining to conclusion (1). This conclusion is concordant with the principal conclusion of Baker, and with the early surmise of Steltzner. Detailed elaboration of the evidence pertaining to conclusion (2) is planned for a subsequent paper. The aerodynamic evidence as described herein is grouped into three divisions:

- (i) External sculpture.
- (ii) Internal distortion of glass stria.
- (iii) Aerodynamic stability of australite shapes.

These divisions are discussed separately in subsequent sections.

In order to obtain first-hand observations of the detailed sculpture of tektites, the senior author has been privileged to examine many of the major tektite collections in Western Europe and in the United States. Examinations have been made thus far of the following collections:

British Museum, London  
 Naturhistoriska Riksmuseet, Stockholm  
 Universitetets Mineralogisk Museum, Copenhagen  
 Mineralogisch-Geologisch Instituut, University of Utrecht  
 Rijksmuseum van Geologie en Mineralogie, Leiden

Technische Hochschule, Delft  
 Museum National d' Histoire Naturelle (Geologique), Paris  
 Naturhistorisches Museum, Vienna  
 Vatican collection in Castel Gandolfo, near Rome  
 U.S. National Museum, Washington, D.C.  
 Bureau of Economic Geology, University of Texas, Austin

The statements made herein about tektite sculpture are based primarily on personal examination of these particular collections.

Of the various tektite collections examined, the most readily recognizable aerodynamic features were found among Dunn's collection of australites in the British Museum, and among Von Koenigswald's collection of Java tektites in Utrecht. Acknowledgment is gratefully made here both to Dr. Max Hey of the British Museum, London, and to Professor G. H. R. von Koenigswald of the Mineralogisch-Geologisch Instituut, University of Utrecht, for their most courteous cooperation in providing access to their respective tektite collections, and for their kind permission to photograph various tektites and meteorites which are reproduced in this report.

### EXTERNAL SCULPTURE

The detailed sculpture of tektites from all the different areas in which they are found generally is extremely varied and complex. The Australian tektites and some of the Java tektites, however, exhibit a sculpture which is comparatively regular and simple. In the present section attention is confined to the button-type sculpture of the australites, and to a related type of sculpture of certain Java tektites. Both of these types are axially symmetric, and hence relatively amenable to experimental investigation. In a later section some consideration is given to the aerodynamics of australite shapes other than the round form buttons.

### RING-WAVE FLOW RIDGES ON AUSTRALITES, JAVANITES, AND METEORITES

A unique characteristic of tektite sculpture—which the experiments described in this section show to be reproducible by aerodynamic ablation—is the presence of ring-wave flow ridges on one side of certain tektites from Australia and Java. These flow ridges sometimes form a spiral

ring, and sometimes a series of concentric rings. Photographs are presented in figure 1 which illustrate the ridges on two australite round buttons, on two australite oval buttons, and on two Java tektites. It is of pertinent historical interest to note here that these curious ring-wave ridges were clearly exhibited on the first Australian tektite described in the scientific literature (ref. 16)—an oval button (quite similar to the ones shown in fig. 1) given to the eminent naturalist Charles Darwin during the Australian stopover of the now famous 1832-36 voyage of the H.M.S. Beagle. From his examination of the oval button, Darwin believed that it was a volcanic bomb, and that its curious configuration was formed from a soft, spinning glass as it was cooled by its motion at a modest velocity through the air. We shall see subsequently that ring-wave flow ridges are formed under different circumstances than Darwin antici-

pated, namely, from a rigid, nonrotating glass as it is heated and ablated by extreme aerodynamic friction from hypervelocity motion relative to the surrounding air. In the century following Darwin, decisive experiments on the shaping of tektite glass remained absent, and his association of the ring waves with a soft spinning body has continued implanted in the minds of some scientists.

A relatively easy way to observe the formation of ring-wave flow ridges is to expose in a wind stream a glass composed of organic, rather than inorganic molecules. When glycerin, for example, is rapidly frozen in liquid nitrogen, it supercools to form a rigid glass. In a conventional supersonic wind-tunnel stream this organic glass is difficult to distort by aerodynamic pressure, but is easy to ablate by aerodynamic heating. Glycerin glass flows readily at room temperature, whereas tektite glass and other glasses composed of inorganic molecules require very high temperatures to flow readily. Some photographs taken in 1959 of glycerin glass ablating at ambient stagnation-point temperature in the Ames 1- by 3-Foot Supersonic Tunnel No. 2 are shown in figure 2. Air flow is from left to right, and increasing time is from top to bottom. The stagnation-point pressure was 1 atm (reservoir pressure, 2 atm), and the Mach number, 3. Prominent ring waves are seen to propagate radially away from the stagnation point. When one compares these ring waves on ablating glycerin glass (fig. 2) with those on Australian tektite glass (fig. 1), a suspicious similarity appears. Notice of this particular similarity was, in fact, the impetus that initiated the present research on tektites.

Experimental facilities in which aerodynamic ablation of inorganic glass can be investigated must operate at temperatures of several thousand degrees Kelvin. In order to heat inorganic glasses to a point where the kinematic viscosity—and hence the flow characteristics—are similar to those of glycerin at room temperature, ordinary soda-lime glass must be heated to about 1900° K, borosilicate glass (pyrex) to about 2100° K, and tektite glass to about 2400° K. Ablation at these higher temperatures can be achieved in current laboratory facilities either by employing a light-gas gun to launch a glass model through stationary air at a hypervelocity, or by employing an electric arc-heated device to launch air over a stationary glass model at a stagnation enthalpy corresponding to

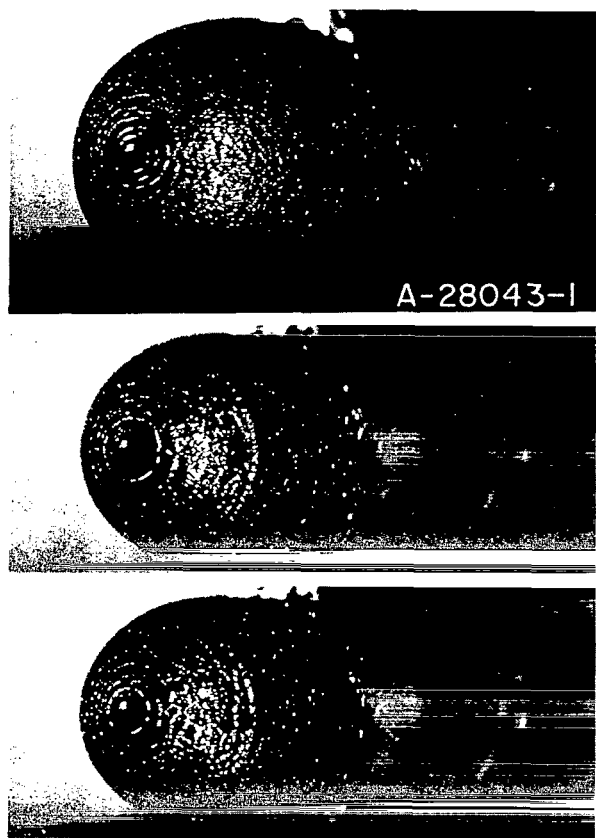


FIGURE 2.—Ring-wave flow ridges on glycerin glass during ablation in the Ames 1- by 1-Foot Supersonic Wind Tunnel No. 2; Mach number 3; reservoir pressure, 2 atm; reservoir temperature, 295° K; approximately normal scale.

a hypervelocity. In the present experiments the Ames concentric-ring electric-arc supersonic jet, described by Shepard and Winovich (ref. 17), was employed to ablate various inorganic glasses. This device provides contamination-free flow at variable pressures.

A visual impression of the manner in which tektite glass ablates in the arc jet may be obtained from figure 3. At the top is a sketch of the method of mounting spherical glass models prior to ablation. The various photographs were taken at different stages in the ablation of a synthetic tektite glass sphere. A white-hot glass layer which flows slowly downstream from the stagnation region can be seen to develop with increasing time ((a) to (e) in this series of photographs). In (a) the arc has just been struck in the chamber; a faintly luminous gas cap is visible but the glass surface temperature has not yet risen to a luminous state. In (b),

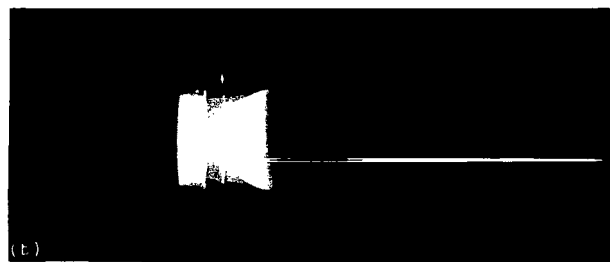
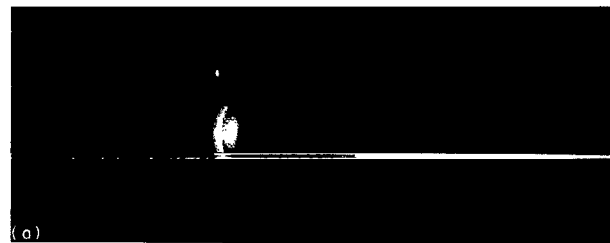
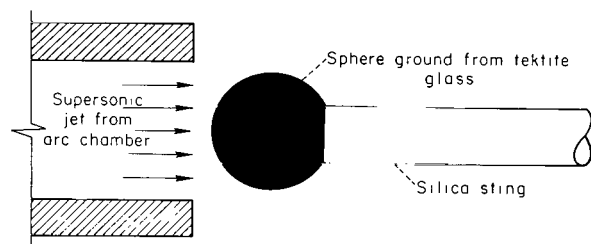
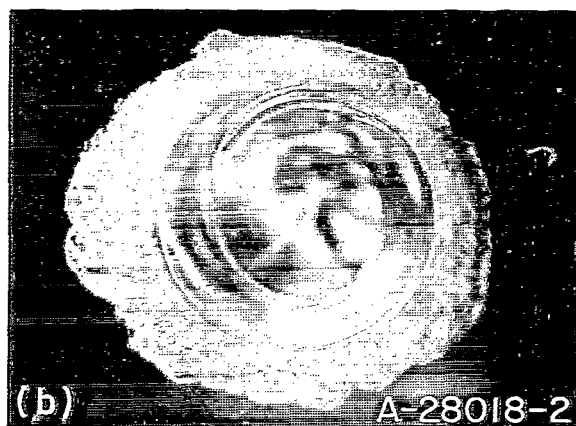
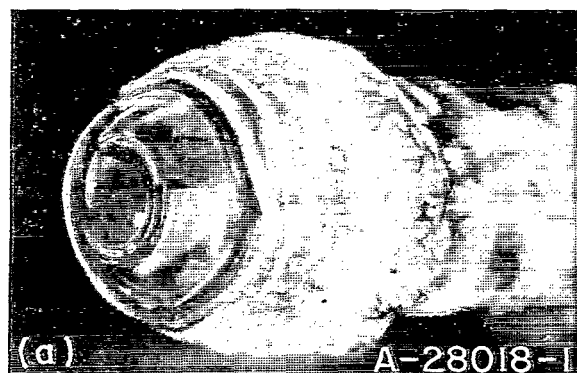


FIGURE 3. Concluded.

several seconds later, the front hemisphere has been heated to incandescence, thereby illuminating the nozzle exit; the white-hot glass near the stagnation region is starting to flow. In (c) the melt flow has accumulated to a diameter approximately equal to the original sphere diameter (1.9 cm) and in (d) it has developed to a circumferential flange of diameter greater than the original sphere. In (e) the arc has just been extinguished after operating for about 20 seconds; the faintly luminous gas cap and bow-shock wave no longer are visible, and the hot glass is solidifying from its rapid cooling. This stage corresponds to the final ablation stage in an entry trajectory wherein the aerodynamic heating rate drops so fast due to decreasing velocity, that the molten glass near the stagnation region begins to be cooled, rather than heated, by aerodynamic friction.

Various experiments in the arc jet have shown that ring-wave ablation patterns like those observed with glycerin are not peculiar just to organic

FIGURE 3.—Sketch of test setup in arc jet, and photographs taken during ablation of 1.9-cm diameter sphere of synthetic tektite glass.



(a) Soda-lime glass;  $\frac{3}{4}$  front view.

(b) Borosilicate glass; front view.

FIGURE 4.—Ring-wave flow ridges on  $\frac{1}{2}$ -inch-diameter glass rods ablated in arc jet.

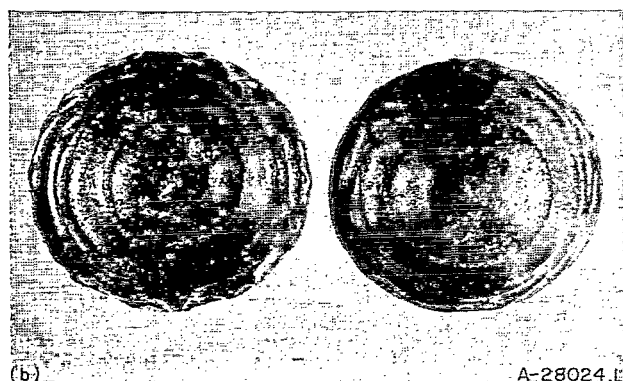
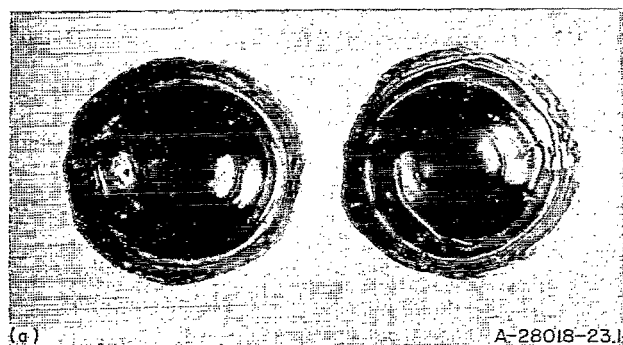
glasses, but are common also to the inorganic glasses such as soda-lime, borosilicate, and tektite glass. Two typical ablation patterns from the arc-jet experiments are shown in figure 4. These were obtained by placing  $\frac{1}{2}$ -inch-diameter glass rods in the arc jet for 10 to 15 seconds with the rod axis aligned parallel to the stream direction. The stagnation-point heating rate of about 98 cal/cm<sup>2</sup> sec (360 Btu/ft<sup>2</sup> sec) was ample to ablate the glass at an estimated surface temperature of roughly 2000° K. Concentric ring-wave flow ridges can be observed in the top portion of figure 4, which is a  $\frac{3}{4}$  front view of an ablated soda-lime glass rod. A spiral

ring-wave system can be observed in the bottom portion, which is a direct frontal view of an ablated borosilicate glass rod. (In both cases the glass melt suddenly becomes frothy after it flows to a certain distance downstream of the stagnation point where the pressure is low enough for the dissolved gases in the glass to cause the melt to vesiculate.) Many other similar examples of ring-wave flow ridges on soda-lime and borosilicate glasses have been observed.

Ring-wave flow ridges, strikingly similar to those exhibited on Australian tektites, have been produced on both synthetic and natural tektite glass by ablation in the arc jet. Rather than to consume unnecessarily the valuable natural tektites, many of the experiments were conducted with synthetic tektite glass. Two slabs of synthetic tektite glass were procured from the Corning Glass Company under specifications of a composition corresponding to that of the average australite. Models were ground from pieces of the slab into the desired shape for testing in the arc jet. Chemical analysis of the synthetic tektite glass, kindly made by F. Cuttitta and M. Carron of the U.S. Geological Survey, showed it to be very close to the specified composition of average Australian tektite glass (see appendix A for a comparison of the synthetic and natural glass composition). Front views of two ablated shapes produced in the arc jet by hypervelocity aerodynamic ablation of the synthetic tektite glass are shown at the top of figure 5; shown for comparison at the bottom are the corresponding views of two Australian tektites (in the British Museum). The striking similarity between ring-wave flow ridges on artificial and natural tektites is evident, and requires no further comment.

Inasmuch as wavelike flow ridges are produced under conditions of extreme aerodynamic heating, such as are encountered during entry at cosmic velocity into the earth's atmosphere, it might be anticipated that recognizably similar wave patterns also would be exhibited on some meteorites. This expectation is indeed confirmed by observation. In the course of examining the various European and U.S. meteorite collections referred to in the INTRODUCTION, meteorites with wavelike patterns on their fusion crust were continually searched for, and three were found among the hundreds examined: Nedagolla, Orleans, and Bugaldi. Nedagolla is a 4.2-kg iron





(a) Front surface of synthetic tektite glass after aerodynamic ablation in arc jet.

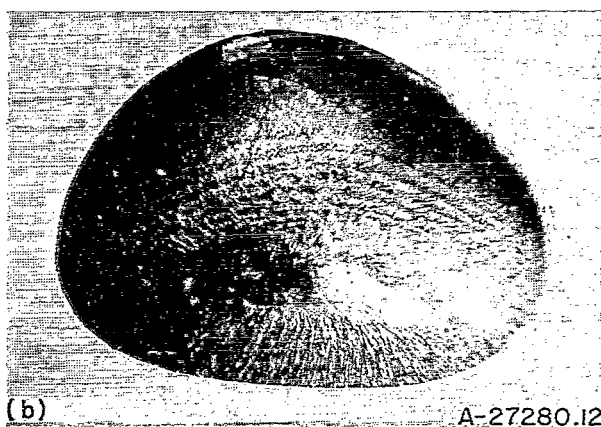
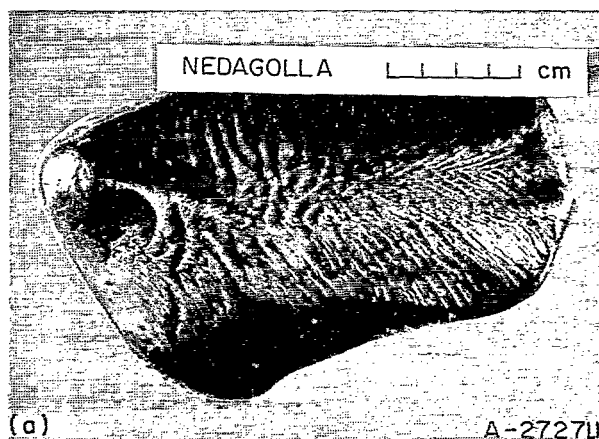
(b) Front surface of Australian tektites; British Museum collection.

FIGURE 5.—Comparison of artificial and natural systems of ring-wave flow ridges.

meteorite which was observed to fall in India and is housed now in the British Museum; it exhibits abundant wavelike flow ridges (fig. 6(a)), though they do not form a simple systematic pattern, presumably as a consequence of the tumbling flight and irregular shape of this meteorite. Orleans (not shown) is a rather large stone meteorite of roughly 25 x 30 x 40 cm dimensions, which fell in France and is now housed in the Vienna Museum; it is one of the relatively few examples wherein tumbling in flight did not occur. Orleans exhibits three thin waves of flow ridges spaced several centimeters apart, disposed essentially normal to the flight direction and situated considerably downstream of the stagnation region. These waves can be traced around most of its

periphery. Bugaldi is a 2-kg iron meteorite which fell in Australia; it is represented in cast form in the British Museum, and exhibits nearly concentric wavelike flow ridges emanating from the stagnation region (fig. 6(b), a photograph of the original).

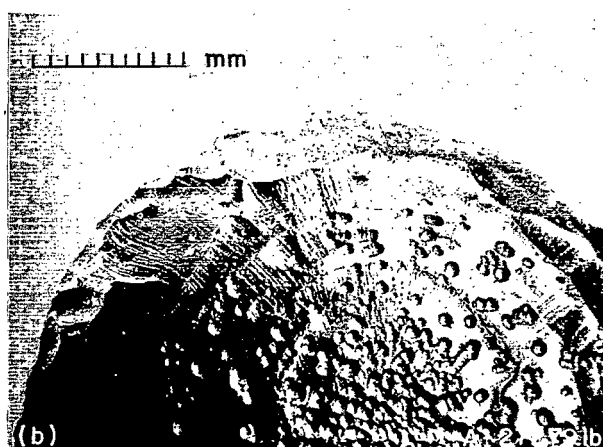
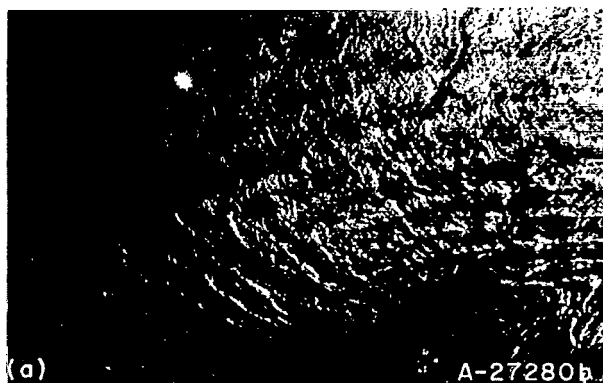
A close examination of surface details reveals, as would be expected intuitively, that the waves in the melted layer have propagated in a direction essentially transverse to the lines of the wave crests. This is the case for both meteorites and tektites. A close-up of the wave pattern on Bugaldi, for example, as shown in figure 7(a), exhibits a number of threadlike streamers which solidified in their path transverse to the waves.



(a) Nedagolla iron, 4.5 kg.

(b) Bugaldi iron, 2 kg.

FIGURE 6.—Meteorites exhibiting wave-like flow ridges on their fusion crust.



(a) Bugaldi iron meteorite.

(b) Hollow button australite.

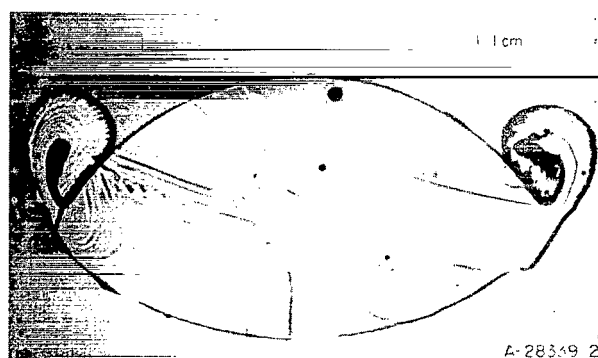
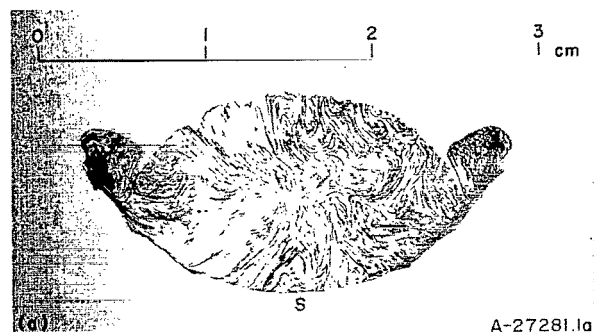
FIGURE 7.—Close-ups of radial flow direction indicators running transverse to wave ridges.

The streamers emanate from the direction of the stagnation region. Thin radial lines emanating from the stagnation point are apparent on the larger Java tektite in figure 1 and are discernible on some of the Australian tektites reproduced therein. These radial flow-direction indicators are more evident on the australite close-up in figure 7(b). This latter tektite was discovered on Kangaroo Island, described by Steltzner (ref. 7), and photographed by Suess (ref. 8). The radial flow lines on tektites do not represent threadlike streamers of melt which have solidified in their tracks—as in the case of the Bugaldi meteorite—but represent glass stria lines just beneath the surface which have been exposed to view by an

etching process during the many millennia of the tektites' terrestrial life. The net result, for both tektite and meteorite, is to show that the surface melt has flowed radially away from the stagnation point in the direction of wave propagation, precisely as is observed in the arc jet when tektite glass ablates under conditions of extreme aerodynamic heating.

#### FLANGES ON AUSTRALITES

Internally coiled flanges are observed around the circumference of tektite glass ablated in the arc jet, just as are observed around the circumference of button-type Australian tektites. That the circumferential flange around australites represents a solidified toroidal vortex of molten glass is clearly revealed by meridional thin sections of tektites (Dunn (ref. 2), Baker (ref. 18)). An excellent example of this is reproduced in figure 8(a), taken from plate X of Baker's treatise



(a) Meridional thin section of australite button (Baker).

(b) Meridional thin section of tektite-glass model ablated by aerodynamic heating.

FIGURE 8.—Sections illustrating coiled circumferential flange on Australian tektite and on tektite-glass model ablated in arc jet.

(ref. 14). The orientation of this section is such that aerodynamically stable flight would be vertically downward in the figure, and the stagnation point would be at the intersection of the front surface and the polar axis. For purposes of comparison a thin section of a tektite glass model ablated in the arc jet is shown correspondingly oriented in figure 8(b). Internal coiling is evident in the circumferential flange of the model subjected to hypervelocity ablation. Due to the radial air flow outward from the stagnation point, the aerodynamic shear and pressure-gradient forces act in the direction compatible with the observed direction of turning within the flange. It is noted that the shape of the glass model of figure 8(b) originally was a lens when placed in the arc jet; a lens corresponds to the shape which would exist in flight at the instant after a flange was shed from a tektite that originally was a sphere before entry into the atmosphere. The flanges on most australites represent second generation (or higher) accumulations of melt.

While it is evident that the artificial product exhibits flange coiling similar to the natural tektite, some of the details of the coiling are not the same between the two. Fine differences in details of striae coiling are not significant, as no two australite flanges are alike in such details, but the over-all difference in flange shape is significant. The flange base is round on the artificial tektite, whereas it is rather flat on the australite. This difference is to be expected from the difference in relative body force in the two cases. The artificial flange was produced in a vertical arc jet wherein the gravitational body force was insufficient to counteract the natural tendency of surface tension to form round flanges. The australite flange, according to the atmosphere-entry analysis of Chapman (ref. 15), was produced under flight conditions wherein the deceleration body force at the time ablation terminated was between one and two orders of magnitude greater than the earth gravitational force. Under such conditions, surface tension is much less important, and the flange bases so formed would be expected to be flatter than those formed under laboratory conditions.

It is of relevant interest to note here that the arc jet experiments did not produce coiling of the flange melt at the lower range of ablation tem-

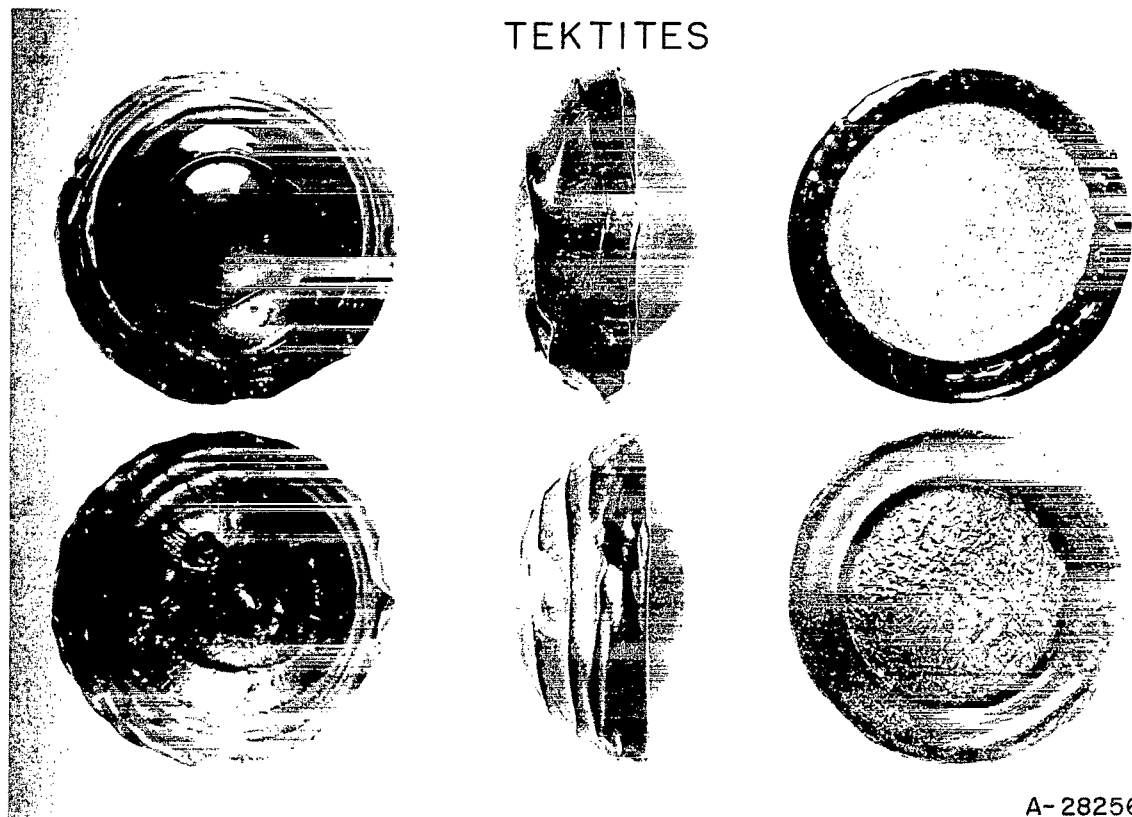
peratures investigated. When the glass flow was relatively viscous and slow moving, it usually accumulated in a few successive laps of thick melt; this type of flange formation was observed when the ablation surface temperature at the stagnation point was less than about  $2000^{\circ}\text{K}$  (e.g., when the viscosity of tektite glass was greater than about that of honey at room temperature). At somewhat higher temperatures of about  $2100^{\circ}\text{K}$ , the accumulating melt folded into a flange, thereby producing a coarse coil of essentially only one turn. The numerous coiled striae displayed in thin sections of australite flanges indicate a history of repeated vortical entwinings, and hence a development from hotter and considerably less viscous melt than that produced in the present experiments. For the calculated conditions of australite entry into the earth's atmosphere, the temperature of ablation is in the range of about  $2500^{\circ}$  to  $2800^{\circ}\text{K}$ , depending on the entry angle and tektite size; these higher temperatures are consistent with the observation of a more entwined coiling in the flanges on tektites from Australia than in the flanges on models from the present experiments.

#### COMPARISON OF NATURAL AND ARTIFICIAL TEKTITE SCULPTURE

A summary comparison of the sculpturing obtained on three different tektite glass models ablated in the arc jet with that exhibited on three different Australian tektites housed in the British Museum is presented in figure 9. Artificial products are on the left, and natural tektites on the right. All are shown enlarged to a common size. Their actual diameters vary somewhat, being 21, 16, and 22 mm, respectively, for the artificial tektites shown in front, side, and base view and 25, 24, and 23 mm, respectively, for the corresponding natural tektites. The principal features of congruity in sculpture between natural australites and arc-jet artifacts are visible here: the common presence of ring-wave flow ridges (front view at left in fig. 9), and the common existence of a rolled-up toroidal flange around the circumference (side and base views in fig. 9).

#### DISTORTION OF INTERNAL GLASS STRIAE

In addition to the conformity in external shape between Australian button tektites and aerodynamically ablated glass, there also exists a



A-28256

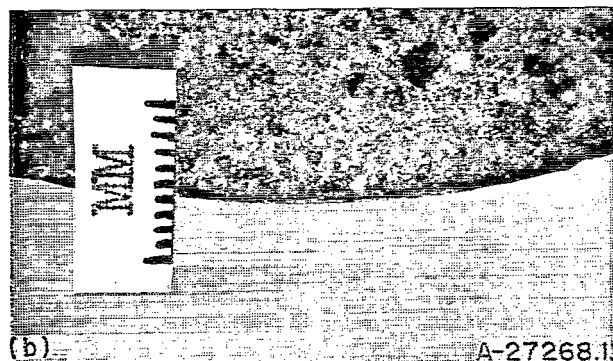
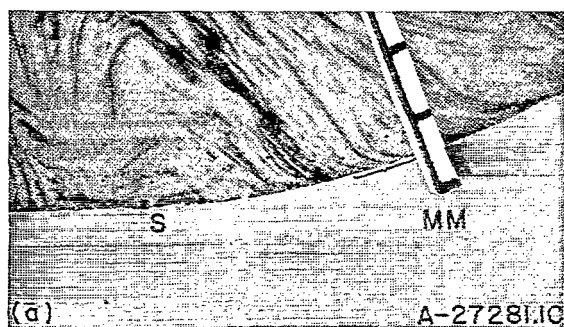
FIGURE 9.—Comparison of three Australian button tektites (at bottom, now in British Museum) with three tektite glass models (at top) ablated by aerodynamic heating.

conformity in internal structure. It has been long known that the australites were twice melted (Fenner (ref. 19), Baker (ref. 14)), the first time when parent tektite material was fused to form primary glass bodies, and a second time when these bodies were superficially heated in a special manner that left an internal record of its occurrence within a thin layer beneath the front face of the australites. The first heating left an irregular, contorted striae pattern within the central-body portion (see fig. 8(a)). The second heating left the striae pattern within the thin frontal layer distorted in a very systematic fashion (see lower surface in fig. 8(a), a close-up of which is presented in fig. 10(a)). As will be seen, these systematic distortions are characterized by the same mathematical functions as those required by the theory of hypervelocity glass ablation, and are the same as those produced in the arc-jet experiments. To extract evidence from the characteristic thinness of this layer and to draw significance from the particular

mathematical form of its systematically distorted striae is the design of the present section.

#### RESULTS FROM ANALYSES OF GLASS ABLATION

The mathematical analysis for aerodynamic ablation of glasses is in a sufficiently advanced state of development to provide an explanation of the systematic alterations exhibited just beneath the front surface of the better preserved australites. When a rigid glass ablates under conditions of extreme aerodynamic heating, the only region substantially affected at a given instant is a thin layer beneath the front surface, as sketched in figure 11. The aerodynamic forces induce rapid radial motion of melted glass outward from the stagnation point, removing by liquid convection the rapid energy input by aerodynamic heating. An analysis appropriate for determining accurately the amount of glass convected away during ablation would require thorough consideration of the relatively complicated transient phenomena encountered during atmosphere entry. However, an



(a) Close-up of thin layer of second period melting on australite button illustrated in figure 8(a).

(b) Thin fusion crust on Ashdon stone meteorite.

FIGURE 10.—Thin layer of second-period melting on australite, and thin fusion crust on stone meteorite.

analysis appropriate for revealing (1) the characteristic thinness of the aerodynamically heated glass layer, and (2) the functional shape of the distorted glass striae can be much simpler. The relatively simple equations for quasi-steady glass ablation, as developed by Bethe and Adams (ref. 20) and by Adams, Powers, and Georgiev (ref. 21), can be adapted for these two limited purposes. Some details of their analysis as applied to australite entry are discussed in appendix B. Here only the end results are considered.

The characteristic thickness  $\delta$  of the melt layer in the stagnation-point region for quasi-steady ablation under conditions wherein the heat radiated from the glass is small compared to the heat convected into it, is given by the equation

$$\delta = \frac{K}{v_{\infty} n} \quad (1)$$

where  $K$  is the thermal diffusivity of the glass,  $v_{\infty}$  is the rate of ablation (velocity of recession of stagnation point), and  $n$  is a dimensionless number characteristic of the glass and dependent on the slope of the viscosity-temperature curve; for tektite glass,  $n$  is about 10. The above equation tells us, as would be expected, that the lower the thermal diffusivity  $K$ , the thinner the melted layer. Of more significance to the present discussion is the result that, for heating rates typical of those encountered during orbital entry, the layer is very thin. An "order of magnitude" consideration for button type australites, such as represented in figure 10(a), will serve to illustrate this point. The primary shape of such australites was a sphere of about 1 cm radius, for which the duration of ablation during entry into the earth's atmosphere at parabolic velocity and at a  $30^\circ$  angle to the horizon, for example, is the order of 10 seconds (it would be somewhat shorter for a vertical entry, and somewhat longer for a shallow entry). Since the amount of ablation at the stagnation point, as determined from the differ-

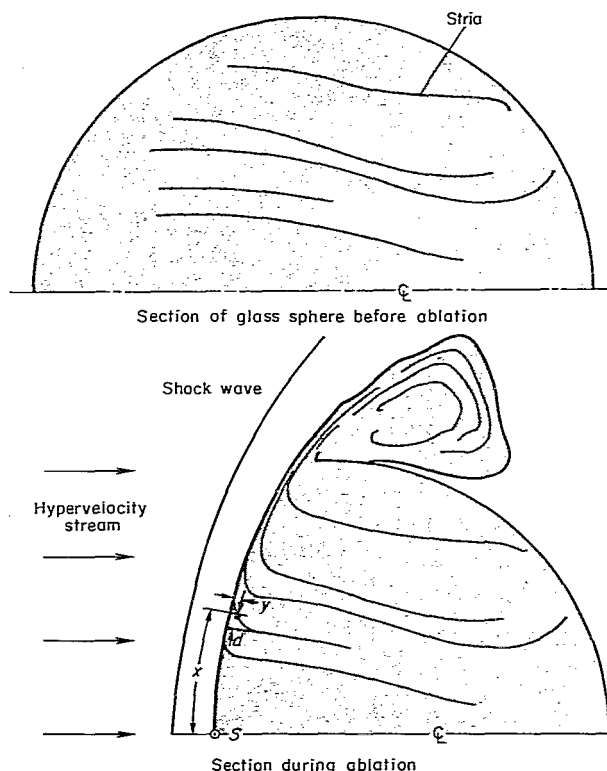


FIGURE 11.—Distortion of internal striae by aerodynamic ablation.

ence between original and final dimensions, is the order of 1 cm,  $v_w$  would be of order 0.1 cm/sec. The thermal diffusivity of tektite glass ( $K$ ) is of order 0.01 cm<sup>2</sup>/sec, and  $n$ , as noted previously, is of order 10. Hence,  $\delta$  from equation (1) is of order 0.01/0.1(10)=0.01 cm, or a tenth of a millimeter. Since  $\delta$  represents the distance in which the melt flow velocity decreases by a factor of 2.718 (see appendix B), it follows that a fundamental characteristic of aerodynamically ablated glass is that the entire flow of fluid glass is convected away in a thin layer only a few tenths of a millimeter thick. Unless the convected liquid adheres by surface tension to the glass core in the form of a flange, the only aerodynamically distorted striae remaining with the tektite would be confined to this thin layer.

In analyzing striae distortions within the frontal layer of tektites, it must be recognized that a small amount of glass has been removed from the surface of even the best preserved australites by chemical etching and mechanical abrading over many millennia of terrestrial exposure. The stria displacement  $d$ , defined by the sketch in figure 11, is an integral of the melt flow velocity  $u$  parallel to the front surface. From the analysis developed in appendix B,  $u$  in the inner portion of the melt layer varies nearly exponentially with  $y$ , the depth below the fresh surface just after ablation, and linearly with  $x$ , the distance from the stagnation point:

$$u \sim x e^{-y/\delta} \quad (2)$$

If the unknown amount of terrestrial erosion is  $y_0$ , and the exponential factor  $e^{-y/\delta}$  is written  $e^{-y_0/\delta} e^{-(y-y_0)/\delta}$ , it is readily seen that, at any given  $x$  where  $y_0$  is fixed, the glass flow velocity  $u$  varies exponentially with depth  $(y-y_0)$  below the eroded surface, as well as exponentially with depth  $y$  below the original fresh surface. The logarithmic decrement  $\delta$  is the same for the two variations. Thus the amount of terrestrial erosion does not affect the determination of  $\delta$  as long as a sufficient portion of the aerodynamically distorted striae still remains.

By focusing attention on the inner portion of the thin layer distorted by aerodynamic heating, the melt velocity component normal to the surface may be treated as sensibly constant, and the striae displacement  $d$  turns out to be nearly proportional to the velocity  $u$ . In the outer portion,

very near the original fresh surface, the normal velocity component varies markedly, and  $d$  varies with  $u$  in a manner more complicated than simple proportionality (see appendix B). In the inner portion, however, which is the only portion remaining on weathered australites, there results

$$d \sim x e^{-y_0/\delta} e^{-(y-y_0)/\delta} \quad (3)$$

It follows that the variation of striae displacement with depth for a given  $x$ , where a fixed but unknown amount  $y_0$  has been eroded, would be simply

$$d \sim e^{-(y-y_0)/\delta} \quad (4)$$

where  $(y-y_0)$  is the depth below the existing eroded surface. By assuming that the erosion was constant over the stagnation region, the striae displacement  $d_0$  at the existing surface ( $y=y_0$ ) would vary according to equation (3) simply as

$$d_0 \sim x \quad (5)$$

In summary, theoretical characteristics of glass ablation by aerodynamic heating require that the ablating region be confined to only a very thin layer (eq. (1)), and that the striae displacements within the inner portion of this layer vary approximately exponentially with depth (eq. (4)), and linearly with distance from the stagnation point (eqs. (3) and (5)).

#### THIN AERODYNAMICALLY HEATED LAYERS ON TEKTTES AND METEORITES

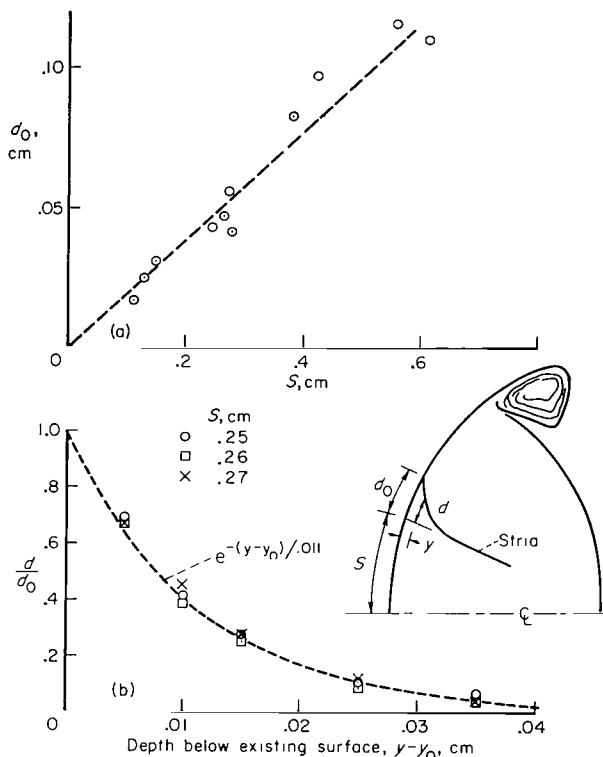
A layer of thinness comparable to that expected from theoretical considerations is exhibited near the front surface of the better preserved australites. An illustration of this is given by the section reproduced in figure 8(a). From the close-up of a portion of this section in figure 10(a), the layer of systematic distortions is seen to be about 0.2 to 0.3 mm thick. In view of the above calculations of  $\delta$ , the observed thinness of this layer shows that the second-period heating rate was of a magnitude comparable with that which would ablate 1 cm of tektite glass in the order of 10 seconds. Aerodynamic ablation rates of such magnitude correspond to flight velocities well into the orbital range.

A thin layer of aerodynamically fused material is also exhibited on meteorites—objects known to have undergone rapid aerodynamic ablation

during hypervelocity entry into the earth's atmosphere. Since meteoritic stone, like tektite glass, has a relatively low thermal diffusivity, the rapid ablation leaves only a thin fusion crust over the meteorite exterior. A typical example illustrating this is presented in figure 10(b), a photograph of a sliced portion of the Ashdon chondrite in the British Museum. The cut was from a region of the front surface; it is of special aerodynamic interest since Ashdon is one of the few meteorites which retained a fixed orientation without tumbling during entry. The fusion crust which separated incandescent air from unaffected stone is seen to be only about 0.4 mm thick. Judging from the comparably thin layer exhibited on the front surface of the australite (fig. 10(a)), we should not be surprised that it too has entered the earth's atmosphere at a very high velocity.

An explicable difference in appearance exists between the aerodynamically heated layers on meteoritic stone and on tektite glass. The thin heat-altered layer on meteorites differs both in color and in physical state from the interior material; certain of the stone minerals were liquefied, oxidized, and darkened as they were heated by the air, and then solidified into a semiglassy state when cooled rapidly. The correspondingly thin layer on australites, however, exhibits the same color and same physical state as its interior material; tektite glass is a mixture of oxides, and, being already oxidized and already in a supercooled liquid state, does not change its chemistry or color when heated in air, nor its physical state when cooled rapidly. Consequently, the evidence of past aerodynamic heating on meteorites is visible openly on the surface, but on tektites it is concealed subtly within the internal structure of distorted glass striae.

A comparison of the striae displacements observed in australites with the calculated displacements for aerodynamic ablation is quite revealing. From photographic enlargements of the thin section in figure 8(a), various measurements were made of  $d_0$ , the striae displacement at the surface. In figure 12(a) the results are plotted as a function of the distance  $s$  measured along the surface from the stagnation point to the striae location before the distortion occurred. The latter location was determined from an extrapolation in the manner illustrated by the sketch accompanying figure 12(b). Each data point in this figure



(a) Surface displacement of glass striae.

(b) Displacement of glass striae beneath surface.

FIGURE 12. Variation of internal displacement of glass striae.

represents one stria exhibiting a clearly defined displacement. Referring to equation (5) we see that during aerodynamic ablation the surface striae displacement  $d_0$  would vary linearly with distance from the stagnation point, and hence linearly with  $s$  which is equal to  $x_0 - d_0$ . As figure 12(a) illustrates, a linear variation is in accordance with the australite data. A plot of the variation in striae displacement with distance  $y$  beneath the surface, for the same australite, is presented in figure 12(b). In this figure the dashed curve represents the simple exponential variation expected within the inner portion of the melt layer for distortions produced by aerodynamic heating. The three types of data points represent the three prominent glass striae situated fairly near each other in the area bracketed in figure 10(a). Here again the observed displacements of internal glass striae within this Australian tektite are in full accord with the required displacements

for hypervelocity aerodynamic ablation of a rigid glass.

A confirmation of the analytical variation of striae displacement  $d$  with depth  $y$  has been obtained from ablation experiments in the arc jet. In figure 13 a photomicrograph is presented of the striae distortions near the front surface of a tektite glass model, ground from an australite, and then ablated in this facility. An exponential type of variation is suspected from a glance at the photomicrograph, and is confirmed by the plot in figure 14. The measured distortions indicated by data points correspond to the most prominent stria in figure 13, and agree well in the inner portion of the layer with the simple exponential variation. In the outer portion, very near the surface ( $y < 0.01$  cm, approximately), the measured displacement departs from the simple exponential in the expected manner, but agrees well with the more complicated function derived in appendix B. The logarithmic decrement of  $\delta = 0.01$  cm over the exponential portion in this particular case is so close to that of the australite ( $\delta = 0.011$  cm), and the striae displacements are so similar to those of the australite (bracketed region in fig.

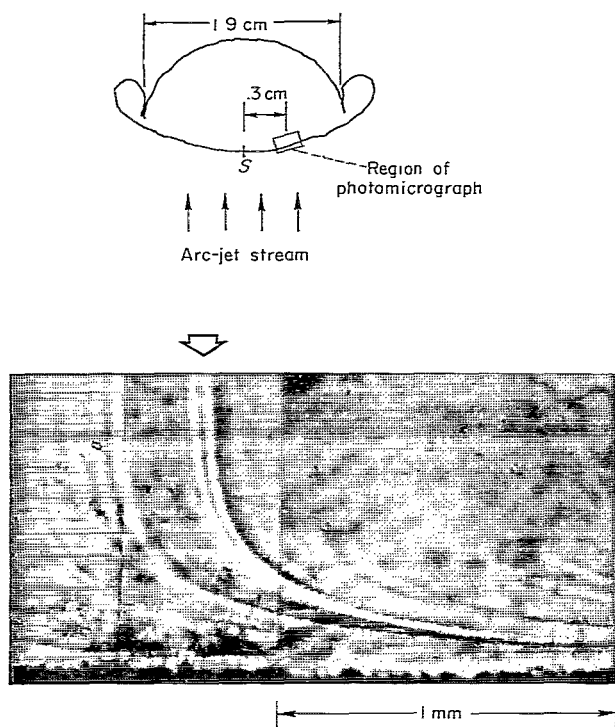


FIGURE 13.—Photomicrograph of striae distortions near surface in thin section of tektite glass ablated in arc jet.

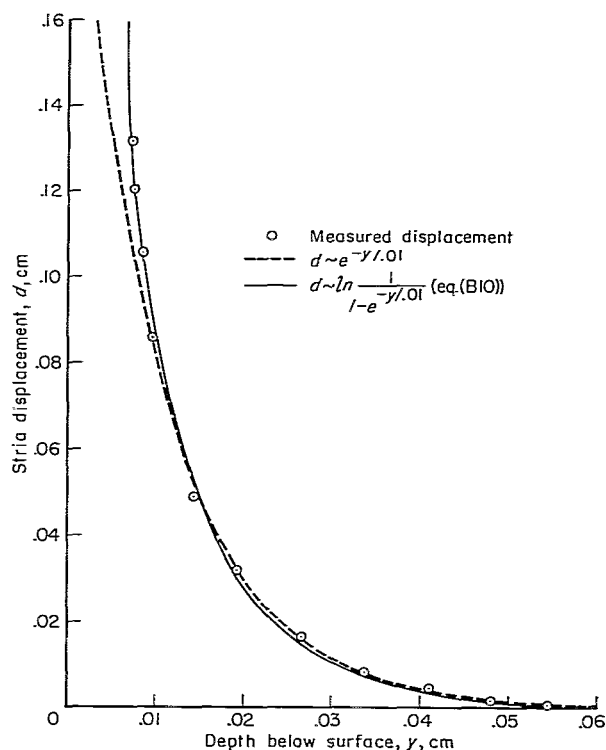


FIGURE 14.—Comparison of stria displacement measured on tektite glass ablated in arc jet with exponential variation.

10(a)), that a direct comparison of the two can be fairly made. Such a comparison, as shown in appendix B, indicates that approximately 0.12 mm of glass has been removed from the front surface of this particular australite, undoubtedly by the etching and eroding agents to which it has been subjected during the many years of its terrestrial exposure.

The photomicrograph in figure 13 corresponds to a model that was ablated under temporally varying test conditions: as time progressed during this run, the velocity of the arc jet was decreased steadily while the pressure was increased simultaneously. Temporally varying conditions of this type exist during an entry flight. The exponential distortions of glass striae also have been observed in models that were ablated under constant test conditions.

The existence of systematic striae distortions confined to a very thin layer beneath the front surface of australites, represented by an exponential variation with depth below the front surface, and by a linear variation with distance from a



unique point, show that the ablation was by aerodynamic heating on a rigid glass, and not by aerodynamic pressure on a soft glass (the latter would have distorted striae systematically to depths of millimeters or centimeters, instead of the tenths of millimeters observed). Any apprehension that a rare coincidence may be involved in the single australite analyzed here disappears when the congruity of tektite shapes with aerodynamically ablated glass is recalled, and when the remarkable aerodynamic stability of the Australian tektite configuration is considered, as explained in the section which follows.

#### AERODYNAMIC STABILITY OF AUSTRALITES

It is the purpose of this section to survey some statistics on the classification of australite shapes, to record the percentage of aerodynamically stable ones, and to explain the reason for the remarkably high incidence of admirable aerodynamic configurations found among these tektites.

While there are many thousands of australites, there are only a relatively few categories of shape into which almost all of them may be classified. These are sketched in figure 15. The tabular values that follow are based on a classification of about 8,000 australites by Baker (ref. 22) from the combined Victorian, Nullarbor Plain, and Charlotte Waters areas:

	Type	Percent
Round forms-----	{ Lenses-----	55.2
	{ Buttons-----	15.6
	{ Ovals-----	13.2
	{ Cores-----	.7
Elongated forms-----	{ Boats-----	6.8
	{ Dumbbells-----	2.0
	{ Canoes-----	1.3
	{ Teardrops-----	2.7
	{ Discs-----	1.1
Total classified forms-----		98.6
Aberrant forms-----		1.4
Grand total-----		100.0

These nine shape groups are seen to comprise 98.6 percent of all complete forms studied. The remaining 1.4 percent represents aberrant forms, such as "crinkly tops," "bowls," and "aerial bombs" that are not readily amenable to aerodynamic stability studies. It is noted that australite fragments are not included in the tabulation above inasmuch as the complete form of which they are a part often is uncertain.

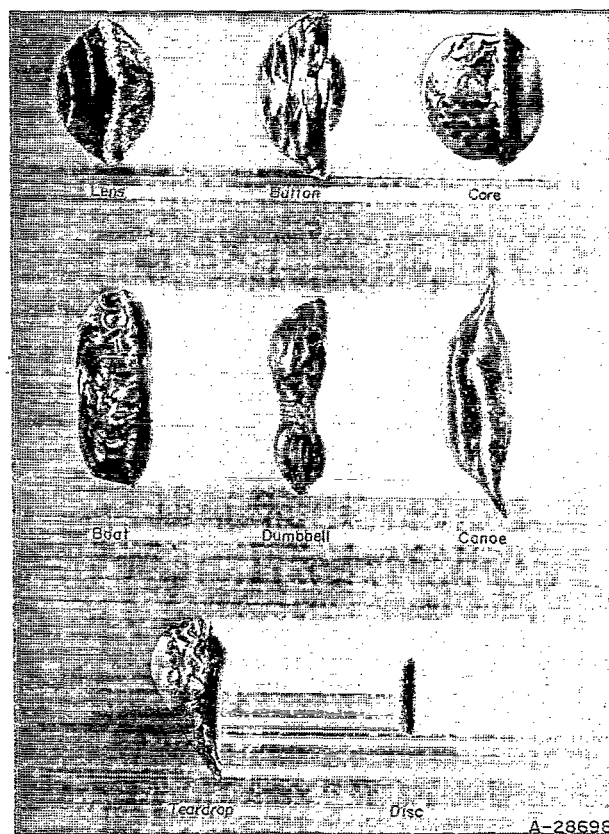


FIGURE 15.—Sketch of principal australite shapes (side views).

For purposes of discussing aerodynamic stability, several of the australite shape categories can be combined. Lenses, for example, are merely buttons with flanges broken off (Fenner (ref. 19), and Baker (ref. 14)). Several stages in the fragmentation sequence of button to lens are illustrated by the specimens photographed in figure 16. While perfect buttons are found rarely, buttons with flanges partially broken off (e.g., base view (a) in fig. 16) are found more frequently, though still only occasionally, whereas lenses without any appreciable flange attached (e.g., side view (b) and four specimens in the lower row of fig. 16) are found commonly. This preponderance of lenses is readily understandable in view of the precariously thin neck connecting flange to lens core, so thin that complete flanges (e.g., (c) in fig. 16) sometimes have separated cleanly from their central body and are found intact.

Insofar as qualitative considerations of aerodynamic stability are concerned, the round forms can be combined with ovals. Thus, the first

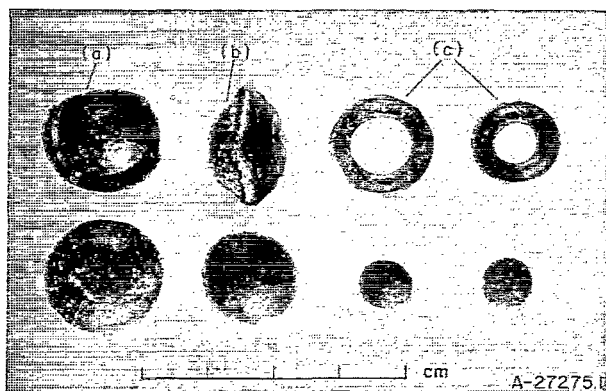
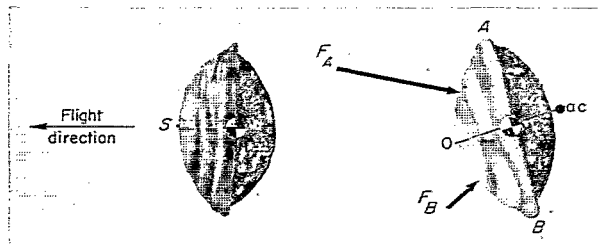


FIGURE 16.—Various stages in the fragmentation of buttons into lenses; from australites in British Museum collection.

three shape categories listed above (lenses, buttons, and ovals), comprising 83.9 percent of the total, are represented in cross section by the following sketch. The ring-wave pattern serves to identify the front surface, to locate the stagna-



tion point  $S$ , and to fix the australite orientation relative to the direction of motion. Configurations such as sketched are known to possess a high degree of static stability in pitch and yaw, although none in roll. The aerodynamic frictional forces acting over the front surface, as well as all forces acting on the base, are entirely negligible compared to the normal pressure forces on the front face. Hence only the latter need be considered in illustrating why such a configuration would tend to return stably to the orientation sketched at the left if it were accidentally disturbed to the orientation sketched at the right. Because the front arc of each meridional section of these particular australites is nearly that of a circle, the vectors representing normal-pressure distribution all pass through a common aerodynamic center point  $a.c.$  which is well aft of the center of gravity  $c.g.$  Also, the integrated force  $F_A$  acting on the upper half  $OA$ , which is disposed

relatively normal to the stream, is larger than the corresponding force  $F_B$  acting on the more inclined lower half  $OB$ . Hence the unbalanced pitching moment about the  $c.g.$  tends to restore the displaced attitude to its original position, and the configuration is statically stable (to a high degree, in fact).

For objects of tektite shape there is little inherent aerodynamic damping, and a statically stable configuration of the lens or button type can fly with oscillatory motions that are either of convergent, divergent, or constant amplitude, depending on the flight trajectory. A detailed exposition of the reasons for this is given by Allen (ref. 23) and Tobak and Allen (ref. 24). Only their end results are utilized here. If a statically stable australite were to ascend along an exit trajectory from the atmosphere, for example, divergent oscillations would be expected; if it were to fly horizontally with steady velocity, constant-amplitude oscillations would be expected; however, if it were to descend along an atmosphere-entry trajectory, rapidly convergent oscillations would be expected. The transient aerodynamic forces which can rapidly diminish oscillations during a descending entry act like a damper, although not as a consequence of any viscous dissipation or of any inherent aerodynamic damping. This damping-like effect of the temporally increasing aerodynamic forces is loosely termed "dynamic stability" herein; it exists during the initial portion of an entry trajectory prior to the attainment of peak deceleration. A close analogy to this effect would be the diminishing oscillations exhibited by a spring-mass system when the spring restoring force increases with time. Once peak deceleration has passed (when the velocity is reduced to roughly half the entry velocity), dynamic instabilities could reappear before the entry is completed. As it turns out, though, the ablation of a highly refractory material like tektite glass, when entering the earth's atmosphere at near parabolic velocity, occurs during the early portion of the entry and finishes about the time peak deceleration is reached. Under these conditions ablation occurs when the aerodynamic forces increase rapidly with time and thereby provide dynamic stability to the statically stable shapes. Consequently, the 83.9 percent of australites which are either lenses or buttons, round form or oval, represent configurations that would be aerodynamically stable during

the ablative portion of a descending flight into the atmosphere.

The high aerodynamic stability pertains to angular motion about any axis normal to the flight direction; aerodynamic forces would provide no stabilization or damping of a rotation around the flight-path axis. Whatever angular momentum about the trajectory axis which a tektite may have before entry would be essentially conserved during entry; hence a possible rolling motion of the buttons and lenses cannot be dismissed from consideration of aerodynamic stability alone. Any roll component to the motion must have been small, however, as Baker (ref. 14) notes, since the striae flow lines on the front surface of australites are radial and not helical.

The aerodynamic stability of australite shapes during the later stages of an entry trajectory need not be of concern here. At the point in an entry trajectory where ablation of tektite glass ceases, the velocity would still be well in the hypersonic regime. As the velocity continues to decrease, and the supersonic, transonic, and subsonic regimes are successively passed through, the australite shape may indeed become unstable, or perhaps even tumble, but such behavior at these lower velocities would not be reflected in the shape found on the ground. The glass melted by aerodynamic heating would have been solidified before any dynamically unstable conditions associated with lower speeds could be encountered.

Turning now to a different shape category, the cores, representing 0.7 percent of the classified shapes, Fenner (ref. 25) has shown that these are nothing more than fat lenses which have had some material spall away from the equatorial and front regions. A fat lens is aerodynamically stable, just as is a thin lens, though to a lesser degree. Oval cores exhibit their equatorial spalling symmetrically around their longest periphery, in harmony with the orientation required for stable flight.

In regard to the elongated shapes—the boats, dumbbells, and canoes—it should be noted at the outset that the complete forms in this category exhibit either a second-period melting pattern, or a related spallation pattern, disposed over their broad face, and never, for example, over a narrow end. Three views of a flanged dumbbell are shown in figure 17, to illustrate this point. The observed patterns are precisely the same as would

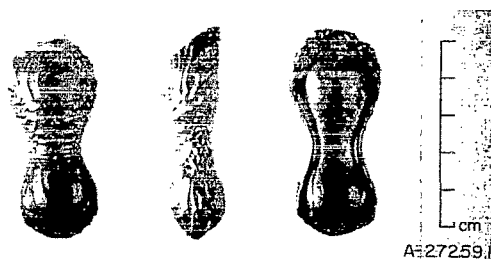
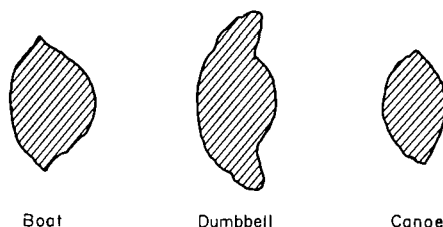


FIGURE 17.—Dumbbell australite with complete flange; from Dunn's collection in British Museum.

be expected from aerodynamically stable flight at a hypervelocity. If the axis of the elongated form were accidentally aligned in the flight direction, it would be highly unstable and forced back to the stable attitude of high drag wherein both the long dimension and the broad face are normal to the flight direction. Some typical cross sections transverse to the long dimension of elongated forms, as figured by Baker (ref. 14), are as follows (flight direction from right to left):



These sections reflect the same features of aerodynamic stability as the corresponding section of lenses and buttons, namely, a nearly circular front of such curvature as to place the aerodynamic center well aft of the center of gravity. Thus, the elongated forms, comprising 10.1 percent of the total, represent aerodynamically stable configurations, just as do the buttons and lenses. While the stabilizing aerodynamic forces would oppose any inclination of the long axis toward the direction of flight, as well as any pitching motion of this long axis, they would not oppose a rolling-type motion about the flight-path axis. Some of the elongated forms may have flown in the fashion of a slowly turning propeller. Evidence that the helix angle must have been small, however, is given by the absence of any spiral component to the flow pattern on the front face. On the elongated form illustrated in figure 17, the flow ridges are very clear, but give no suggestion of a spiral component; they do indicate, however,

that the slightly larger end of this dumbbell leaned a little into the stream. A slightly leaning attitude of this type is, in fact, the aerodynamically stable orientation for such a configuration.

Complete australite teardrops and disc forms also exhibit a pattern of second-period melting which is fully compatible with aerodynamic expectations. A teardrop in hypervelocity flight will trim with its axis inclined to the flight direction at an angle which is dependent on the length-diameter ratio. There are no cases known to the authors in which a second-period melt pattern, or a secondary spallation pattern, is disposed about a teardrop in a manner that would imply motion in an aerodynamically unstable attitude, such as pointed nose first. Similar comments apply to the disc forms. They have clearly experienced a second-period melting in the aerodynamically stable attitude for a disc, namely, with disc axis parallel to, and broad face facing, the flight direction. Tektite discs with rounded edges are statically stable in hypervelocity flight, and hence dynamically stable while ablating during an entry trajectory.

From the above it is seen that the nine principal shape types, comprising 98.6 percent of the complete forms classified, represent configurations which would be aerodynamically stable when entering the atmosphere in the unique attitude which is compatible with the particular second-period melt pattern observed on each type. This remarkable score contrasts drastically with the corresponding score for meteorites, only a few percent of which have traversed the atmosphere as aerodynamically stable objects. The prevalence of stable australites is attributable partly to their regular shapes before entry, and partly to the inherently stable forms which such shapes take on as soon as ablation begins. The many thousand well preserved australites clearly reveal that they were formed from primary shapes which are figures of revolution. (See Fenner (ref. 19) and Baker (ref. 14).) Initially most were spheres, a shape which has no preferred aerodynamic orientation until ablation begins. If a sphere were initially turning about some axis, it would continue to turn until melting started at some point. As soon as the melt flowed back, however, the decreased curvature of the front, and the accompanying rearward movement of the aerodynamic center, would result in a preference for

the orientation which happened to exist when ablation began. Any turning motion existing at this time would be converted into a rapidly subsiding wobble by the stabilizing action of the aerodynamic forces; some of the australite buttons with spiral ring waves may correspond to such cases.

#### CONCLUDING REMARKS

A past history of extremely high aerodynamic heating rates on the Australian tektites is revealed by (1) the presence of ring-wave flow ridges and coiled circumferential flanges which are reproducible in the aerodynamic laboratory, by (2) the existence of a very thin layer—as thin as the fusion crust on meteorites—of systematically distorted glass striae which also are reproducible in the aerodynamic laboratory, and which are describable through precisely the same mathematical functions as appear in the theory of aerodynamic ablation, and by (3) the character of their external shapes, almost all of which, when oriented in the particular manner that is compatible with the attitude demanded by the ring waves and flow lines on the front face, represent configurations of static and dynamic stability during a *descending* entry into the atmosphere. These features constitute conclusive evidence that the australites have entered the earth's atmosphere as *rigid* glass objects and have experienced ablation by extreme aerodynamic heating in hypervelocity flight.

Certain of the Java tektites also exhibit trademark features of aerodynamic ablation. A thin, smooth, semiglossy layer on one side only of an otherwise rough or bubble-pitted tektite has been observed by the senior author on over a hundred small javanites in the collection of G.H.R. von Koenigswald. Because of their small size (generally less than 1 cm diameter), only the largest few exhibit ring-wave flow ridges. They do not exhibit circumferential flanges; these require a certain combination of special shapes, special sizes, and special entry conditions not generally to be expected. Many javanites, however, exhibit on the semiglossy layer the telltale radial flow lines emanating from a central point which is coincident with the stagnation point for stable aerodynamic flight. Other evidence for a second heating of the javanites, as noted by Von Koenigswald (refs. 26, 27, 28, and especially ref. 11), is contained on some fragments possessing one surface sculptured like a

meteorite and rounded at the edges, suggesting fragmentation during flight. In this connection, it appears relevant that Barnes (ref. 29) recently has observed in thin sections of two javanites (and also one indochinite) a demarcated surface layer of strain, which he interprets as evidence of a second heating. The over-all evidence leaves no doubt that the Java tektites, as well as the Australian tektites, have experienced ablation from severe aerodynamic heating.

Decisive evidence of aerodynamic ablation is apparent today in only a portion of the various tektite groups. To the authors' knowledge, no bediasite or moldavite, for example, exhibits evidence which demonstrably is aerodynamic in origin. Barnes (refs. 29 and 30) and Krinov (ref. 1), among others, have concluded that the sculpture of these tektites is attributable to chemical and mechanical erosion. Such a conclusion, however, definitely does not exclude the possibility that these two tektite groups, like those from Australia and Java, have entered the earth's atmosphere at a hypervelocity and have experienced aerodynamic ablation sometime in the past. The great age of these tektites and the characteristic thinness of an aerodynamically ablated layer provide an explanation for this possibility. From measurements of the amount of radiogenic potassium and argon, Gentner and Zähringer (ref. 31) have deduced an age of 29 million years for the bediasites, and 9 million years for the moldavites. Studies of the geological environment of these tektites have indicated even older ages. It is to be expected, then, that any record of aerodynamic ablation, which necessarily is confined to a thin surface layer, and which once may have covered the bediasites and moldavites, would long ago have been obliterated by agents of chemical and mechanical erosion acting over their many million years of terrestrial exposure. The absence today of aerodynamic sculpturing on such ancient tektites does not preclude an aerodynamic past. Conversely, the presence today of aerodynamic sculpturing on only a portion of the younger tektites, which have a common radiogenic age of 0.6 million years, and which are found in Australia, Indonesia, Indochina, South China, and the Philippines, does not preclude the presence of such sculpturing on all of them at sometime in the past; even the best preserved group of these younger tektites — the australites — are worn

enough and old enough that terrestrial agents in most cases have either dimmed or removed the thin outer layer to which aerodynamic evidence is confined.

From the vantage point attained now through direct experimental evidence, a clear picture can be formulated of the physical conditions which produced the remarkable sculpturing on the Australian tektites. In comparing this picture with the multitude of theories advanced in past and current literature, the various nonaerodynamic hypotheses may be disregarded, and, among the various aerodynamic hypotheses, several misconceptions of the ablation process may be perceived and clarified. One misconception stems from the assumption that tektite ablation can be described by the equations developed for meteor physics. Because of their relatively small size and high entry velocity, most meteors ablate mainly by evaporation in free molecule flow, whereas the larger and slower australites have ablated mainly by melting in laminar continuum flow. Since the physical processes are entirely different for these two types of ablation, and since the heating rates for the two types of flow (at the pertinent Reynolds numbers involved) are of different orders of magnitude, calculations which are based solely on the equations of meteor ablation are not applicable to tektites. By the use of such equations in reference 12, for example, it has been concluded incorrectly that tektite ablation takes place mainly by evaporation. Actually, the mass of tektite glass evaporated (determined from balance measurements in the present experiments) is small compared to the mass melted, as required by the calculations of australite ablation in laminar continuum flow (ref. 15). Other misconceptions concern the supposition that the australites either were soft when sculptured by the air, or were slowly heated, deeply melted, and thereby ablated in a manner essentially different from that of meteorites: in the past, without experiments on aerodynamic ablation to serve as a guide, it has been hypothesized, for example, that the australite shapes were sculptured by the air from masses of soft glass shed from the ablation of a large body (Hardcastle (ref. 32), Lacroix (ref. 9), and Fenner (ref. 10)); that, in contrast to meteorites, they were formed from such a deep heating during flight that the aerodynamic forces molded the glass

like a plastic (Nininger (ref. 33)); and that they were shaped from a long and slow heating in a grazing entry of a few minutes duration which heated the australites to much greater depths than meteorites (O'Keefe (ref. 12)). However, a synthesis of the new experimental evidence with the applicable theoretical evidence, and with the previous observational evidence of Baker (ref. 14), leads with assurance to a picture of the aerodynamic sculpturing conditions which are similar to those encountered during a direct entry flight

of a small, relatively slow meteorite: the structural state of the body is firmly rigid, the rate of heating is extremely high, the recession of the front face is rather rapid, the duration of the ablation is relatively short (seconds to tens of seconds, rather than a few minutes), and the penetration of the melting at any given instant is confined to a very thin, receding sheet of fluid glass.

AMES RESEARCH CENTER

NATIONAL AERONAUTICS AND SPACE ADMINISTRATION

MOFFETT FIELD, CALIF., *Oct. 16, 1961*

## APPENDIX A

### COMPOSITION OF SYNTHETIC TEKTITE AND AVERAGE AUSTRALITE GLASS

In the following table figures are given for the composition of two different pieces taken from a slab of synthetic tektite glass and analyzed by F. Cuttitta and M. Carron of the U.S. Geological Survey. "Average australite" designates the desired composition specified to the Corning Glass Company. All numbers represent weight percentages of the various oxides.

	<i>Average australite</i>	<i>Analyses of synthetic tektite glass</i>	
SiO <sub>2</sub> .....	76. 0	75. 64	75. 77
Al <sub>2</sub> O <sub>3</sub> .....	11. 0	11. 36	11. 46
Fe <sub>2</sub> O <sub>3</sub> .....	. 5	. 50	. 60
FeO .....	4. 5	4. 44	4. 23
CaO .....	3. 0	3. 09	2. 88
MgO .....	1. 5	1. 61	1. 62
MnO .....	. 1	. 10	. 10
Na <sub>2</sub> O .....	1. 0	1. 04	1. 00
K <sub>2</sub> O .....	1. 9	1. 88	1. 89
TiO <sub>2</sub> .....	. 5	. 49	. 49
P <sub>2</sub> O <sub>5</sub> .....	0	. 02	. 02

It is evident that the synthetic tektite glass employed in the experiments represents closely the average australite.

## APPENDIX B

### ANALYTICAL RESULTS PERTAINING TO THE AERODYNAMIC ABLATION OF GLASS

An important physical feature characterizing the aerodynamic ablation of glass is that the depth of the surface layer within which the melt runs off is much less than the depth of the layer within which the temperature rise has penetrated. The strong dependence of glass viscosity on temperature is responsible for this feature. With tektite glass, for example, the viscosity increases an order of magnitude when the temperature drops only about 200° C. Since the surface temperature of ablation is roughly 2000° C above the interior glass temperature, it is clear that the velocity profile of liquid flow  $u(y)$  will extend beneath the surface to a depth about one order of magnitude less than that to which the temperature profile  $T(y)$  extends. This means that, in the development of equations for the systematic striae distortions induced by ablation, only a small portion of the over-all temperature profile need be considered. In this portion, very near the surface, the temperature is approximated by an exponential

$$T - T_0 = (T_w - T_0) e^{-y/\Delta} \quad (\text{B1})$$

with

$$\Delta = \frac{T_w - T_0}{\left(\frac{dT}{dy}\right)_w} \quad (\text{B2})$$

where  $T$  is the internal temperature at a distance  $y$  beneath the surface,  $T_0$  is the temperature before heating occurred,  $T_w$  is the wall temperature, and  $(dT/dy)_w$  is the slope of the temperature profile at the wall. It may be noted that Bethe and Adams (ref. 20) employed the exponential function for  $T$  throughout the entire temperature profile.

Another important feature of glass ablation is that the equations of momentum conservation and of mass conservation are the same for transient ablation as for steady-state ablation. This situation exists because the time-dependent inertia terms in the momentum equation are negligible compared to the shear and pressure terms, and because the time-dependent term in the continuity equation also is negligible for incompressible fluids such as glass. Therefore, although we are concerned here with a transient phenomenon, the

solution to the momentum equation for the velocity profile may be taken directly from that of Bethe and Adams who considered explicitly only steady-state ablation.

$$u = \frac{\delta e^{-y/\delta}}{\mu_w} \left[ \tau_w - \delta p' \left( 1 + \frac{y}{\delta} \right) \right] \quad (\text{B3})$$

with

$$\delta = \left[ -\frac{T_w - T_0}{\mu_w} \left( \frac{d\mu}{dT} \right)_w \right] = \frac{\Delta}{n} \quad (\text{B4})$$

where  $\mu_w$  is the viscosity at the surface temperature  $T_w$ ,  $\tau_w$  is the aerodynamic shear stress at the glass-air interface, and  $p'$  is the surface pressure gradient. The exponential  $e^{-y/\delta}$  dominates the righthand side of equation (B3), so that  $\delta$  may be regarded as the characteristic thickness of the flowing layer of glass. For most inorganic glasses, including tektite glass, the viscosity varies so rapidly with temperature that the quantity

$$n = \left[ -\frac{T_w - T_0}{\mu_w} \left( \frac{d\mu}{dT} \right)_w \right]$$

is the order of 10. It follows directly from equation (B4) that  $\delta$  is an order of magnitude less than the characteristic thickness  $\Delta$  of the temperature profile.

The distortion  $d$  parallel to the surface, illustrated schematically in figure 11, is related to the melt velocity components  $u$  parallel, and  $v$  perpendicular, to the surface

$$d = \int_y^\infty \frac{u(x, y, t)}{v(x, y, t)} dy \quad (\text{B5})$$

For tektite glass, the vaporization is negligible compared to the melting at entry flight conditions near the termination of ablation, so that the Bethe-Adams equation for  $v$  is

$$v = \frac{2\delta^2}{\mu_w} [(\tau_w' - 2p''\delta)(1 - e^{-y/\delta}) + p''ye^{-y/\delta}] \quad (\text{B6})$$

By introducing a parameter dependent on flight conditions

$$A = \frac{-p''\delta}{\tau_w' - 2p''\delta} \quad (\text{B7})$$



the integral in equation (B5) becomes, with  $\xi$  as the dummy variable for  $y/\delta$ ,

$$d = \int_{y/\delta}^{\infty} \frac{x e^{-\xi} [1 - A(1 - \xi)]}{2[1 - e^{-\xi}(1 + A\xi)]} d\xi \quad (\text{B8})$$

By employing a mean value  $\bar{x}$ , intermediate between the undisturbed coordinate ( $s$ ) and the displaced coordinate ( $x$ ) of a given particle, the integral of equation (B8) reduces to the form

$$\frac{d}{\bar{x}} = F\left(\frac{y}{\delta}, A\right) = \frac{1}{2} \int_{y/\delta}^{\infty} \frac{e^{-\xi} [1 - A(1 - \xi)] d\xi}{[1 - e^{-\xi}(1 + A\xi)]} \quad (\text{B9a})$$

$$= -\ln \sqrt{1 - e^{-y/\delta} \left(1 + \frac{Ay}{\delta}\right)} \text{ for } A = \text{constant} \quad (\text{B9b})$$

which should be a good approximation when  $d \ll s$ .

In principle, this integral for striae displacement would be cumbersome to evaluate precisely, since  $A$  is a complicated function of time, but, for the small values of  $A$  appropriate to tektites, the above integral is not sensitive to the exact value of  $A$ , or to moderate variations in  $A$ , so long as  $A$  remains sufficiently small. For entry objects the size of a typical australite, for example,  $A$  increases from a very small value at the beginning of ablation to about 0.1 or 0.2 at the end of ablation, depending on the entry angle. Under such conditions numerical calculation from the complete equation (B8) shows that the value  $A=0$ , in fact, provides a good approximation through the proportionality relationship

$$d \sim F\left(\frac{y}{\delta}, 0\right) = \ln \frac{1}{\sqrt{1 - e^{-y/\delta}}} \quad (\text{B10})$$

Moreover, for practical purposes, this function differs little from a simple function proportional to  $e^{-y/\delta}$  in the inner portion of the melt layer where  $y/\delta$  is greater than about 1. Even on the better preserved australites the outer portion very near the original ablated surface ( $y/\delta$  less than about 1) has been worn away. Consequently, the entire analysis reduces, in essence, to the simple result that the remaining striae displacements (on all but a perfectly preserved specimen) would be expected to follow the simple exponential variation  $d \sim e^{-y/\delta}$  to a good degree of approximation.

It is to be noted that the striae displacement equation (B9) provides a means of estimating the amount of erosion from the front face if only a

portion of the systematic striae displacements have been worn away. For example, the average surface stria displacement from the data of figure 12(a) corresponds to  $d_0/s \cong 0.20$ , and to  $d/\bar{x} \cong 0.18$ . The corresponding value of  $y_0/\delta$  (from eq. (B10)) which produces this particular value of  $d/\bar{x}$  is about 1.2. Hence, with  $\delta = 0.01$  cm (fig. 12(b)),  $y_0 = 0.012$  cm is the approximate amount of glass that has been removed from the front face of this tektite.

The above analysis, leading to equation (B9b) for the striae displacement  $d/\bar{x}$ , is valid for small displacements; but a similar equation can be developed for large striae displacements. Thus, by considering  $x$  as a variable in equation (B8) (rather than as a constant  $\bar{x}$ ), and by noting that  $d = x - s$ , equations (B8) and (B9) yield

$$\int_s^x \frac{dx}{x} = F\left(\frac{y}{\delta}, A\right) = -\ln \sqrt{1 - e^{-y/\delta} \left(1 + \frac{Ay}{\delta}\right)} \quad (\text{B9c})$$

or,

$$\frac{d}{s} = \frac{1}{\sqrt{1 - e^{-y/\delta} \left(1 + \frac{Ay}{\delta}\right)}} - 1 \quad (\text{B9d})$$

For small displacements the right hand side of this equation reduces to  $e^{-y/\delta} (1 + Ay/\delta)/2$ , as does the right hand side of equation (B9b).

The calculations above are for transient ablation. In the special case of steady-state ablation, as shown by Bethe and Adams, a very simple equation can be developed which is useful in estimating the order of magnitude of  $\delta$ . Because of the smallness of  $\delta$  relative to  $\Delta$ , the sheet of flowing glass may be considered as being convected away at the wall temperature  $T_w$ , carrying with it an energy flux of  $\rho c_p v_w (T_w - T_0)$ , where  $\rho$  is the glass density,  $c_p$  the specific heat, and  $v_w$  is the velocity of recession—or rate of ablation—of the stagnation point ( $v_w > 0$ ). Since  $(dT/dy)_w = -(T_w - T_0)/\Delta$  from equation (B1), it follows that the heat input to a glass of thermal conductivity  $k_w$  is  $k_w (T_w - T_0)/\Delta$ , and, that in the absence of vaporization, the heat balance equation for steady ablation is

$$k_w \frac{T_w - T_0}{\Delta} = \rho c_p v_w (T_w - T_0) \quad (\text{B11})$$

When this is combined with equation (B4), there results

$$\delta = \frac{K}{v_w n} \quad (\text{B12})$$

where  $K = k_w / \rho c_p$  is the thermal diffusivity of the glass. When internal radiation is considered, equation (B12) is modified. For the purpose of

illustrating the order of magnitude of  $\delta$ , however, equation (B11) is adequate.

#### REFERENCES

1. Krinov, E. L.: Some Considerations on Tektites. *Geochimica et Cosmochimica Acta*, vol. 14, 1958, pp. 259-266.
2. Dunn, E. J.: Australites. *Bulletin Geological Survey of Victoria*, no. 27, 1912, pp. 3-23.
3. Urey, Harold C.: Origin of Tektites. *Nature*, vol. 179, no. 4559, Mar. 16, 1957, pp. 556-557.
4. Berwerth, F.: Können die Tektite als Kunstprodukte gedeütet werden? *Centralblatt für Mineralogie*, 1917, pp. 240-254.
5. Watson, Fletcher, Jr.: Origin of Tektites. *Nature*, vol. 136, 1935, pp. 105-106.
6. Hawkins, Gerald S.: Tektites and the Earth. *Nature*, vol. 185, no. 4709, Jan. 30, 1960, pp. 300-301.
7. Steltzner, Alfred W.: Über Eigenthümliche Obsidian-Bomben aus Australia. *Zeitschrift d. Deutschen Geologischen Gesellschaft*, vol. XLV, 1893, pp. 299-319.
8. Suess, Franz E.: Die Herkunft der Moldavite und Verwandter Gläser. *Jahrbuch d. Kaiserlich Königlich Geologischen Reichsanstalt*, vol. 50, 1900, pp. 193-382.
9. Lacroix, M. A.: Les Tectites de l'Indochine, *Archives Museum d'Histoire Naturelle*, Paris, ser. 6, vol. 8, 1932, pp. 139-240.
10. Fenner, Charles: Australites; Part III, A Contribution to the Problem of the Origin of Tektites. *Trans. Roy. Soc. South Australia*, Vol. 62, 1938, pp. 192-216.
11. Von Koenigswald, G. H. R.: Tektite Studies III—Some Observations on Javanese Tektites. *Proc. Koninklijke Nederlandse Akademie van Wetenschappen*, Amsterdam, vol. 64, ser. B, 1961, pp. 200-203.
12. O'Keefe, John A.: The Origin of the Tektites. *Proc. 1st International Space Science Symposium*, North-Holland Publishing Co., Amsterdam, 1960, pp. 1080-1105.
13. Baker, George: The Role of Aerodynamical Phenomena in Shaping and Sculpturing Australian Tektites. *Am. Jour. Sci.*, vol. 256, June 1958, pp. 369-383.
14. Baker, George: Tektites. *Memoirs Nat. Museum Victoria*, vol. 23, 1959, pp. 1-313.
15. Chapman, Dean R.: Recent Re-Entry Research and the Cosmic Origin of Tektites. *Nature*, vol. 188, no. 4748, Oct. 29, 1960, pp. 353-355.
16. Darwin, Charles: Geological Observations on the Volcanic Islands and Parts of South America Visited During the Voyage of H.M.S. Beagle. 1844, republished by Appleton and Co., New York, 1891, pp. 44-45.
17. Shepard, Charles E., and Winovich, Warren: Electric-Arc Jets for Producing Gas Streams With Negligible Contamination. *ASME Preprint 61-WA-247*, 1961.
18. Baker, George: The Flanges of Australites (tektites). *Memoirs Nat. Museum of Victoria*, vol. 14 (1), 1944, pp. 7-22.
19. Fenner, Charles: Australites; Part I, Classification of the W. H. C. Shaw Collection. *Trans. Roy. Soc. South Australia*, vol. 58, 1934, pp. 62-79.
20. Bethe, Hans A., and Adams, Mac C.: A Theory for the Ablation of Glassy Materials. *Jour. Aero/Space Sciences*, vol. 26, no. 6, June 1959, pp. 321-328, 350.
21. Adams, Mac C., Powers, Wm. E., and Georgiev, Steven: An Experimental and Theoretical Study of Quartz Ablation at the Stagnation Point. *Jour. Aero/Space Sciences*, vol. 27, no. 7, July 1960, pp. 535-543.
22. Baker, George: Nirranda Strewnfield Australites, South-East of Warrnamboul, Western Victoria. *Memoirs Nat. Museum Victoria*, vol. 20, 1956, pp. 59-172.
23. Allen, H. Julian: Motion of a Ballistic Missile Angularly Misaligned With the Flight Path Upon Entering the Atmosphere, and Its Effect Upon Aerodynamic Heating, Aerodynamic Loads, and Miss Distance. *NACA TN 4048*, 1957.
24. Tobak, Murray, and Allen, H. Julian: Dynamic Stability of Vehicles Traversing Ascending or Descending Paths Through the Atmosphere. *NACA TN 4275*, 1958.
25. Fenner, Charles: Australites; Part II, Numbers, Forms, Distribution and Origin. *Trans. Roy. Soc. South Australia*, vol. 59, 1935, pp. 125-140.
26. Von Koenigswald, G. H. R.: Tektites from Java. *Akademie van Wetenschappen*, Amsterdam, *Proc. ser. B*, vol. 60, 1957, pp. 371-382.
27. Von Koenigswald, G. H. R.: Tektite Studies II—The Distribution of the Indo-Australian Tektites. *Proc. Koninklijke Nederlandse Akademie van Wetenschappen*, Amsterdam, vol. 63, ser. B, 1960, pp. 142-153.
28. Von Koenigswald, G. H. R.: Tektite Studies IV—Collision Marks on Tektites, "Drop Marks," and "Hollow Tektites," *Proc. Koninklijke Nederlandse Akademie van Wetenschappen*, Amsterdam, vol. 64, ser. B, 1961, pp. 204-219.
29. Barnes, Virgil E.: Significance of Inhomogeneity in Tektites. *Report of International Geological Congress, XXI Session, Norden, Part XII*, Copenhagen, 1960.
30. Barnes, Virgil E.: North American Tektites. *University of Texas Publication, Contributions to Geology*, Part 2, 1939, pp. 477-582.
31. Gentner, W., and Zähringer, J.: Das Kalium-Argon-Alter von Tektiten. *Zeit. f. Naturforschung*, Band 152, Heft 2, 1960, pp. 93-99.
32. Hardecastle, H.: The Origin of Australites; Plastic Sweepings of a Meteorite. *New Zealand Jour. Sci. Tech.*, 8 (2), 1926, pp. 65-75.
33. Nininger, H. H.: *Out of the Sky*. Dover Pub., 1952, p. 308.